Highly Accelerated Life Stress Testing (HALST) of Base-Metal Electrode Multilayer Ceramic Capacitors

David (Donhang) Liu
MEI Technologies, Inc.
NASA Goddard Space Flight Center
Greenbelt, MD 20771
Donhang.liu-1@nasa.gov

Abstract

An improved highly accelerated life stress test (HALST) procedure and modeling method was developed to evaluate the reliability of multilayer ceramic capacitors with base-metal electrodes (BMEs). Reliabilities of ceramic capacitors with precious-metal electrodes (PMEs) and BMEs are discussed. A combination of leakage current and mean-time-to-failure (MTTF) measurements under accelerated life stress conditions have been used to distinguish and separate the MTTF data into two failure groups: slow degradation and catastrophic. The slow degradation failures, characterized by a near-linear leakage increase against stress time, fit well to an exponential model over an applied field. A characteristic exponential growth time, τ_{SD}, is defined to describe the reliability life of this failure mode. The two separated MTTF data groups have been fitted to the *2*-parameter Weibull model. When data points in the catastrophic subset are used for reliability modeling, the data points of the slow degradation subset are treated as suspensions, and vice versa. MTTF of most BME capacitors reveals an exponential dependence on an applied electric field due to the mixed failure modes. The initial MTTF data for slow degradation failures appears to follow the exponential law, and that for catastrophic failures follows the conventional power law. The reliability model developed with respect to mixed failure modes and acceleration factors agrees well with the HALST results -- not only with the MTTF data, but also with the failure modes (catastrophic or slow degradation).

BX life has been used to replace MTTF for evaluating the reliability life of BME capacitors at 125^{o}C and 2x rated voltage (V_r), the condition that all MLCCs are subject to pass at at least 1,000 hours life test for consideration for high-reliability space applications. This B0.8 approach can be used to select BME capacitors that exhibit the potential for passing the life test when evaluated using the quick turnaround HALST method developed in this work.

Introduction

Highly accelerated life testing has been commonly used for the reliability evaluation of MLCCs [1-7]. The testing involves the determination of time-to-failure (TTF) of capacitors at elevated life stress conditions (usually external applied voltage and temperature) that are higher than regular use-level conditions (room temperature and rated voltage, typically). However, highly accelerated life testing results for many BME MLCCs, particularly those with thin dielectric layers, have been found to not always give rise to correct predictions of use-level lifetimes [6,7]. In many cases, the calculated MTTF is longer than that actually achieved through life testing. Several factors may account for this problem: (1) higher accelerated life stresses are often required to generate failures, which results in the introduction of new failure modes. This is especially common for BME capacitors, since the improved microstructure of BME MLCCs will need much higher life stresses to cause a failure in a reasonable period of time, as compared to the conventional PME ceramic capacitors. (2) The failure modes characterized by the Weibull slope parameter β are very likely to change when extrapolating the TTF data at high life stress levels down to the use-level that is normally more than 100^{o}C lower in temperature and several times less in voltage. (3) A statistical method that can handle the multiple failure modes and handle specific acceleration factors needs to be developed. Some studies have indicated that the acceleration factors of BME MLCCs do not always follow the conventional power-law relationship over applied voltage; rather, they likely follow an exponential relationship (*E*-model) [1,8].

Reliability of BME and PME MLCCs

The reliability of an MLCC is the ability of the dielectric material to retain its insulating properties under stated environmental and operational conditions for a specified period of time *t*. The reliability of a capacitor device can be expressed when a *2*-parameter Weibull model is used:

$$R(t) = e^{-(\frac{t}{\eta})^{\beta}} \tag{1}$$

where *e* is the base for natural logarithms, β is the dimensionless *slope* parameter whose value is often characteristic of the particular failure mode under study, and η is the *scale* parameter that represents a characteristic time at which 63.2% of the population has failed and that is related to all other characteristic times, such as mean time to failure (MTTF):

$$MTTF = \eta\Gamma(1 + 1/\beta), \tag{2}$$

where $\Gamma(x)$ is the gamma function of *x* (Note: $\Gamma(1+1/\beta) \approx 0.9$ when $\beta > 3.0$).

Eq. (1) provides a simple and clear understanding of reliability: (1) Reliability is a function of time and always decreases with time, which indicates that the loss of reliability is a common behavior for all devices. (2) Since η and β always exceed zero, the value of *R(t)* is always between 0 and 1, indicating that reliability can also be viewed as the probability of a failure occurring. (3) Reliability typically defines the durability of a system that can function normally. When $\beta > 3$ and $t < \eta$, *R(t)* ~1, suggesting a reliable life span before η. When $t > \eta$, *R(t)* decreases rapidly to 0. The lifetime of a device to sustain its function can be characterized by η, as shown in Eq. (2).

It is widely known that the failure rate for MLCCs that is caused by a single failure mode when both *V* and *T* are changed from V_1 to V_2 and T_1 to T_2 is the product of the separate acceleration factors:

$$A_{VT} = \frac{t_1}{t_2} = \left(\frac{V_2}{V_1}\right)^n exp\left[\frac{E_a}{k}\left(\frac{1}{T_1} - \frac{1}{T_2}\right)\right]. \tag{3}$$

where *n* is an empirical parameter that represents the voltage acceleration factors, E_a is an activation energy that represents the temperature acceleration factor, and k is the Boltzmann constant. This so-called Prokopowicz and Vaskas equation (*P-V* equation) [9] has proven to be useful in the capacitor industry for testing PME MLCCs at various highly accelerated testing conditions. An average of $n \sim 3$ has been found for the voltage acceleration factor, and an average value of $1 < E_a < 2$ eV is typical for the temperature acceleration factor [10-12].

Since only a single failure mode is assumed, the value of β in Eq. (1) should not change over applied stresses. Only the Weibull distribution scale parameter η will change with external stresses. It can be expressed, according to Eq. (3), as

$$\eta(V, T) = \frac{C}{V^n} \cdot e^{(\frac{B}{T})}, \tag{4}$$

where *C* and $B = E_a/k$ are constants.

Therefore, when the external stresses *V* and *T* are both taken into account, the Weibull reliability from Eq. (1) can be expressed again as:

$$R(t, V, T) = e^{-\left(\frac{t \cdot V^n e^{-(\frac{E_a}{kT})}}{C}\right)^{\beta}}. \qquad \text{(For PMEs)} \tag{5}$$

On the other hand, the reliability of an MLCC was also found to be dependent on its construction. This includes an early report that the P-V equation was modified with the active area of internal electrodes [3] and a more general consideration of the number of dielectric layers, dielectric thickness, and average grain size [7]. As a result, the reliability of an MLCC R_t can generally be expressed as:

$$R_t(t, V, T, N, d, \bar{r}, \dots) = \varphi(N, d, \bar{r}, \dots) \cdot R(t, V, T) \tag{6}$$

where *N*, *d*, and $\bar{r}$, are the number of dielectric layers, the dielectric thickness, and the average grain size, respectively.

For PME MLCCs that were qualified for high-reliability applications, a minimum dielectric thickness is always required per MIL-PRF-123, paragraph, 3.4.1. The number of dielectric layers in a PME MLCC typically does not exceed 100. The impact of MLCC construction parameters on the reliability of traditional PME capacitors has been found negligible, and $\varphi(N, d, \bar{r}, \dots) = 1$ for these high-reliability BME capacitors. Therefore, the reliability of PME capacitors with respect to *V* and *T* can generally be expressed by Eq. (5), i.e., a single failure mode with a power-law acceleration factor.

The reliability of BME capacitors is more complicated than that of PMEs. Since the number of dielectric layers can be as high as 1,000, the dielectric thickness d can go from sub-microns to over 10 microns, and since the maximum grain size $\bar{r}$ also varies between 0.2 and 0.8 μm, the impact of construction and microstructure parameters on reliability is not negligible. In a previous study, an empirical relationship was developed to reflect this impact [7]:

$$\varphi(N, d, \bar{a}, \dots) \approx \left[1 - \left(\frac{\bar{r}}{d}\right)^{\alpha}\right]^{N}, \tag{7}$$

where α is an empirical parameter and ≈ 6 for BME capacitors under 50V. Eq. (7) can be better understood if Eq. (6) is rewritten as:

$$R_t(t < \eta) = \left[1 - \left(\frac{\bar{r}}{d}\right)^{\alpha}\right]^{N} \times e^{-\left[\frac{t}{C} \cdot V^{n} \cdot e^{\frac{E_a}{kT}}\right]^{\beta}} \approx \left[1 - \left(\frac{\bar{r}}{d}\right)^{\alpha}\right]^{N} \times 1. \tag{8}$$

This means that when the reliability life of an MLCC is longer than the scale parameter η, the reliability can be simplified to a time-independent term $\varphi(N, d, \bar{r}, \dots)$ and is only determined by the construction parameters and microstructure of a BME capacitor. The simplified reliability form of Eq. (8) has been used to screen out BME capacitors that could never pass the high-reliability requirement for space applications due to their construction and microstructure (*N* is too large, and *d* is too small) [7].

The calculation of reliability for BME capacitors is further complicated because the MTTF of BME MLCCs does not always follow the power law with respect to applied voltage. The deviation of the P-V equation was first observed as early as 1984 for PME capacitors under highly accelerated stresses [1]. J. Scott also reported that the MTTF for (Ba,Sr)TiO_3-based integrated ferroelectrics in memory applications appears to follow an exponential relationship over an electrical field rather than the traditional power-law relationship [13, 14]. Meanwhile, a general *E*-model was proposed by McPherson based on a thermo-chemical model that involves the migration of oxygen vacancies [15-17]. Although the *E*-model was proposed to explain and predict the reliability in SiO_2 gate-oxide, it has recently also been applied to explain the MTTF in BME capacitors due to the similar oxygen vacancy migration behavior [8].

Table I summarizes the three possible acceleration factors that may be applied to explain the BME capacitors' reliability with respect to different levels of *E* and *T*, where $E \approx V/d$ is the electrical field per dielectric layer [17]. When oxygen vacancy migration is involved in the dielectric failures, and when dielectric thickness has changed significantly, each acceleration factor in Table I could be a possibility to fit the actual MTTF data at a given level of external stresses.

Table I. Summary of Acceleration Factors for BME MLCCs [17]

Type of acceleration factors	Expression to scale parameter η	Expression to time-to-failure
E-Model (Low Field)	$\eta(E,T) = Ce^{-bE} \cdot e^{(\frac{E_a}{kT})}$	$\frac{t_1}{t_2} = exp[-b(E_1 - E_2)]exp\left[\frac{E_a}{k}\left(\frac{1}{T_1} - \frac{1}{T_2}\right)\right]$
Inverse Power Law (P-V equation)	$\eta(V,T) = \frac{C}{V^n} \cdot e^{(\frac{E_a}{kT})}$	$\frac{t_1}{t_2} = \left(\frac{V_2}{V_1}\right)^n exp\left[\frac{E_a}{k}\left(\frac{1}{T_1} - \frac{1}{T_2}\right)\right]$
E-Model (High Field)	$\eta(E,T) = Ce^{-A\frac{E}{T}} \cdot e^{(\frac{E_a}{kT})}$	$\frac{t_1}{t_2} = exp\left[-\frac{A}{k}\left(\frac{E_1}{T_1} - \frac{E_2}{T_2}\right)\right]exp\left[\frac{E_a}{k}\left(\frac{1}{T_1} - \frac{1}{T_2}\right)\right]$

Finally, the reliability life of a BME capacitor is further complicated when more than one failure mode is present [6, 7]. For a BME capacitor mixed with *l* independent failure modes, the Weibull reliability Eq. (1) can be extended as:

$$R_t(t) = \left[1 - \left(\frac{\bar{r}}{d}\right)^{\alpha}\right]^N \sum_{m=1}^{l} e^{-\left(\frac{t}{\eta_{m(E(V),T)}}\right)^{\beta m}}. \qquad \text{(For BMEs)} \qquad (9)$$

Where slope parameter $\eta_m(E(V),T)$ can be one of three forms, as shown in Table I.

HALST and Leakage Current Characterization in BME Capacitors

Traditional accelerated life testing requires the collection of a number of MTTF data under various *V* and *T* levels to fit a selected statistical model. The complexity in the reliability of BME MLCCs requires additional test results to be used in order to build up a reliability model. Since leakage current was previously reported to differentiate the failure modes of ceramic capacitors [1], the leakage current as a function of stress time has been in-situ monitored and recorded for each BME capacitor until the capacitor has reached the failure criterion, which is always set at 100 μA for all BME capacitors in this study. A series resistor is also connected to each BME capacitor under test for the purpose of current limiting. The values of the resistors were selected so at least 95% of the applied voltage will be loaded on the BME capacitors. A testing board that contains 20 BME capacitors of a given part number was first tested to determine the failure rate at elevated voltages and temperatures, and to define an test window for which all parts will reach the failure criterion in a reasonable period of time and at external stress levels as low as possible.

Figure 1 shows the measured leakage current as a function of stress time for a 4.7 μF, 16V BME capacitor from manufacturer C (C08X47516) that was tested at 165°C and 72V. All capacitor units revealed a gradual, near-linear increase in leakage current, with some of them followed by a catastrophic dielectric breakdown, characterized by a rapid and accelerated increase of leakage against time. In order to better present the details of the failures, the results shown in Figure 1 have been re-plotted to normalize the leakage data of all capacitors to the failure time of the capacitor with the longest time to failure among 20 units being tested. The corresponding normalized leakage data are shown in Figure 2. It is interesting to note that leakage of most BME capacitors showed a similar slope vs. stress time prior to the beginning of a catastrophic breakdown.

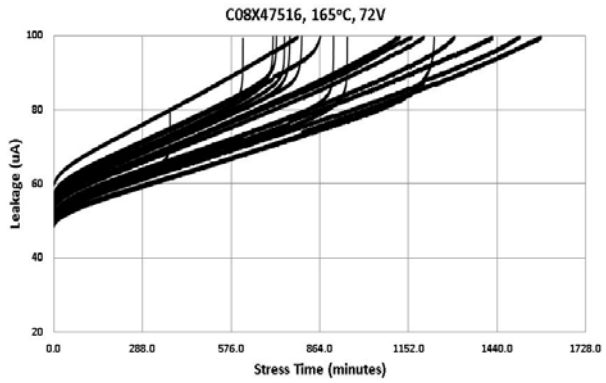

Figure 1. Leakage current of 20 BME capacitors as a function of stress time for a 4.7 μF, 16V BME capacitor from manufacturer C, tested at 165°C and 72V.

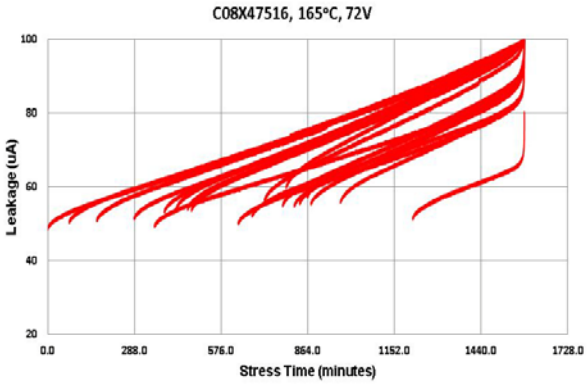

Figure 2. All leakage data from Figure 1 were normalized and re-plotted to the time-to-failure value of the BME capacitor that lasted the longest in the group.

Only two failure modes can be distinguished in Figure 1: catastrophic and slow degradation. Catastrophic failures are characterized by a time-accelerated increase of leakage current that may cause catastrophic damage to the capacitor (either avalanche or thermal runaway). Slow degradation failures are characterized by a gradual, near-linear increase of leakage current against stress time until the failure criterion (100μA throughout this study) is reached. This slow degradation failure has been attributed to the electromigration of ionized oxygen vacancies that gradually reduced the barrier height at the grain boundary regime and caused a gradual leakage current increase, a failure mechanism that is dominant and unique for BME capacitors.

Failure analyses on BME capacitors that failed during HALST [18] revealed that the failure mechanism in $BaTiO_3$ dielectric might be better described by a two-stage dielectric wearout process that initiated with a slow dielectric degradation, followed by a thermally dominated catastrophic breakdown (Figure 3). When the failure criterion is set

with respect to a leakage current level, some BME capacitors will reach the failure level with a catastrophic failure, and some will fail prior to the occurrence of a catastrophic dielectric breakdown.

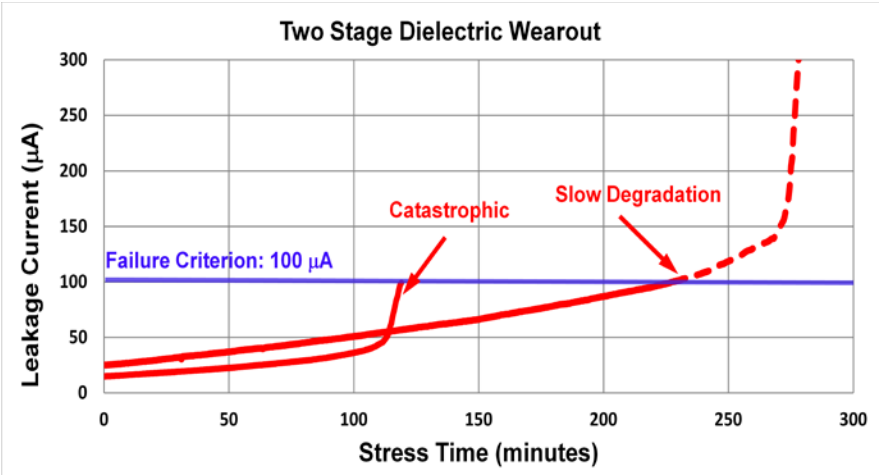

Figure 3. A two-stage dielectric wearout failure mode is proposed for describing the dielectric breakdown behaviors in BME capacitors [18].

A slow degradation failure such as that shown in Figure 3 may be quantified by the slope of a line that connects the onset point of the leakage increase and the failure criterion point at 100 μA. In order to understand this failure mechanism, four different empirical degradation formulas, i.e., linear, power law, exponential, and logarithmic, have been used for curve-fitting the leakage current data, as shown in Figure 4. The curve-fitting coefficient of determination, R^2, has been used to quantitatively determine the validity of the formula that was used. R^2 is most often seen as a number between 0 and 1.0 and is used to describe how well a regression line fits a set of data. An R^2 near 1.0 indicates that a regression line fits the data well, while an R^2 closer to 0 indicates that a regression line does not fit the data at all.

Although the leakage data shown in Figure 2 appear to be linear for most of the time measured, the curve-fitting results show that the exponential form of

$$I_{SD} = I_{SD}(t_0)e^{\left(\frac{t}{\tau_{SD}}\right)} \tag{10}$$

actually fits most of the leakage data better than a linear form, given the relatively higher values of R^2 obtained and the broad range of data that is covered. In Eq. (10), I_{BD} is the measured leakage current, t_0 is the onset time of I_{SD} takeoff, and τ_{SD} is a characteristic exponential growth time. A larger value of τ_{SD} indicates a longer, slower degradation failure. Logarithms do not fit any data well among the formulas.

The following general power-law equation has also been used for curve-fitting the leakage data:

$$I_{SD} = I_{SD}(t_0)[1 + A_0(t)^m],$$

and a linear regression line form was actually used [17]:

$$\left(\frac{I_{SD}}{I_{SD}(t_0)} - 1\right) = A_0(t)^m. \tag{11}$$

Where m is the power-law exponent and t_0 is the time at which all data points taken after t_0 will be used for the curve fitting. Table II compares the curve-fitting results for both exponential and power law on the leakage data that are shown in Figure 2.

Table II. Exponential and Power-Law Curve-Fitting Results of Leakage Current Data in Figure 2

C08X47516, 165°C, 72V			Exponential Fitting Eq. (10)			Power-Law Fitting Eq. (11)		
Position on PCB Board	TTF (minutes)	Failure Mode	τ (Hrs)	I(0)	R^2	Slope *m*	A_0	R^2
C15	377.26	Catastrophic	27.778	25.68	0.979	7.528	3.0E-25	0.849
C12	614.70	Catastrophic	27.778	33.80	0.992	4.832	2.0E-16	0.875
C16	712.00	Catastrophic	27.778	35.08	0.995	5.197	1.0E-17	0.905
C19	723.40	Catastrophic	33.333	37.88	0.996	4.375	6.0E-15	0.888
C14	749.30	Catastrophic	33.333	37.56	0.996	4.679	7.0E-16	0.888
C10	766.34	Catastrophic	33.333	37.48	0.993	3.953	2.0E-13	0.894
C18	793.25	Slow Degradation	27.778	41.48	0.998	4.250	2.0E-14	0.887
C4	805.29	Catastrophic	33.333	38.83	0.994	3.511	4.0E-12	0.898
C17	866.30	Catastrophic	33.333	40.85	0.997	3.476	6.0E-12	0.896
C3	908.27	Catastrophic	41.667	41.72	0.993	3.481	4.0E-12	0.902
C9	953.18	Catastrophic	33.333	39.97	0.994	2.865	5.0E-10	0.908
C2	1112.39	Slow Degradation	33.333	46.82	0.999	2.791	9.0E-10	0.915
C8	1124.51	Slow Degradation	33.333	46.82	0.999	2.865	6.0E-10	0.920
C6	1163.47	Slow Degradation	33.333	47.77	0.999	2.368	2.0E-08	0.924
C0	1203.19	Slow Degradation	33.333	48.51	0.999	2.417	2.0E-08	0.931
C7	1235.54	Catastrophic	41.667	45.56	0.992	1.919	6.0E-07	0.935
C13	1302.47	Slow Degradation	41.667	48.71	0.999	2.138	1.0E-07	0.948
C11	1425.38	Slow Degradation	41.667	51.88	0.999	1.884	8.0E-07	0.951
C1	1515.23	Slow Degradation	41.667	53.51	0.999	1.576	8.0E-06	0.968
C5	1583.30	Slow Degradation	41.667	52.95	0.999	1.293	6.0E-05	0.988

The example of determination of the fitting parameters is shown in Figure 4(a) for a BME capacitor, C13, which revealed a slow degradation failure. Although both exponential and power-law forms yield comparable R^2 values, the leakage current data were fitted almost perfectly to the exponential equation [Eq. (10)], with R^2 very close to 1.

As shown in Table II, the R^2 values decrease when the exponential form of Eq. (10) is used to fit the catastrophic failure data. The catastrophic failure example shown in Figure 4(b) for C7 indicates that the formula only fits leakage data well prior to the beginning of a catastrophic failure.

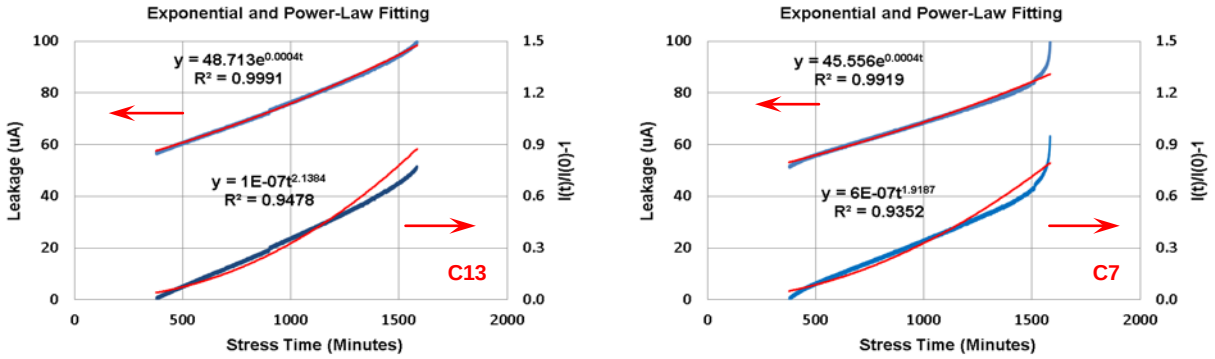

(a) (b)

Figure 4. Exponential and power law curve fitting of leakage data for capacitor sample C13 of Table II as a slow degradation failure example (a) and C7 as a catastrophic failure example (b).

The described curve-fitting process has been performed for all of the leakage current data measured at different stress levels and for different BME capacitors. This practice gives rise to the following conclusions:

(1) Slow degradation failures appear to fit an exponential relationship over stress time. (2) Although the power-law form of Eq. (11) appears to also fit slow degradation failures, with comparable but always lower R^2 values to those of the exponential form of Eq. (10), the power-law relationship appears too aggressive to fit the slow degradation

failures. (3) None of the exponential form or power-law form fits catastrophic data well, indicating that a different failure mechanism must be associated with the catastrophic failures. (4) The meaning of τ_{SD} can be illustrated by the following example: Let I_1 and I_2 be the leakages at t_1 and t_2, respectively, for a slow degradation failure. If one assumes $\frac{I_2}{I_1} = 2$, then Eq. (10) can be rewritten as:

$$\frac{I_2}{I_1} = e^{\left(\frac{t_2 - t_1}{\tau_{SD}}\right)} = e^{\left(\frac{\Delta t}{\tau_{SD}}\right)} = 2, \text{and } \tau_{SD} = \frac{\Delta t}{ln\,(2)} \approx 1.4427 \cdot \Delta t.$$

Where Δt is the time at which the leakage current doubles its value. The greater the τ_{SD}, the longer the time span of a slow degradation failure. τ_{SD} has been found to decrease with increasing stress levels. The development of a physical model that relates τ_{SD} to the microstructure of $BaTiO_3$ dielectrics is in progress.

Weibull Modeling of BME Capacitors with Two-Stage Dielectric Wearout

Figure 5 shows a Weibull plot of a 0603, 0.1 µF, and 25V BME capacitor from manufacturer A (A06X10425) tested at 165°C and 215V. This BME capacitor revealed a dielectric thickness of 7.89 µm and was fabricated for high-reliability evaluations. It took more than 8 times the rated voltage to generate enough failures in a reasonable period of time. Arrows indicate all of the units that failed with catastrophic failures; the remaining units failed with slow degradation. It is important to note that two failure modes, characterized by two different values of slope parameter β, can be clearly distinguished in the Weibull probability plot. Statistically, the data set has to be separated with respect to slope parameter β into two subsets and must fit the Weibull distribution, respectively.

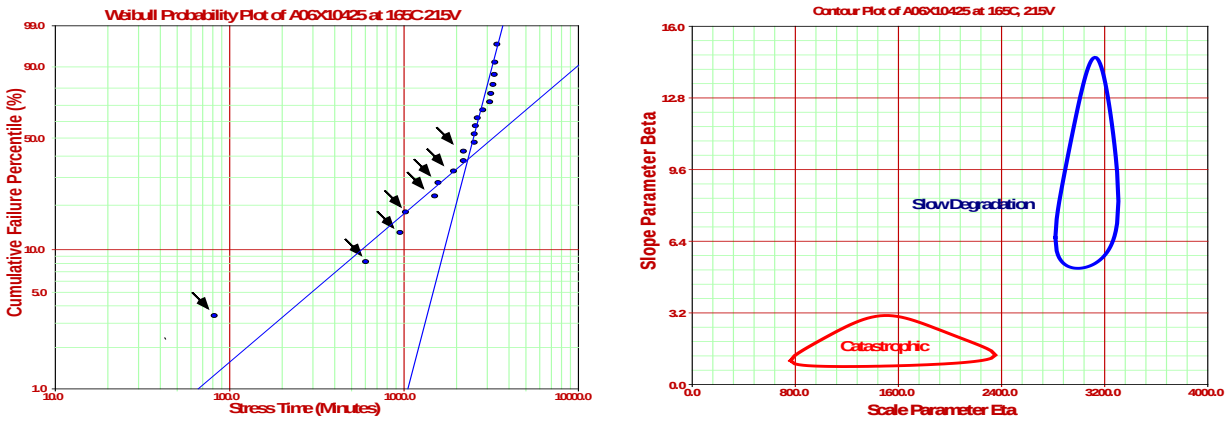

(a) (b)

Figure 5. Weibull modeling results for a 0.01 µF, 0603, 25V (A06X10425) BME capacitor from manufacturer A, life tested at 165°C and 215V. (a) Weibull probability plot, with arrows indicating the catastrophic failures. (b) Corresponding contour plot shows two failure modes that can be statistically separated.

Weibull modeling of the data shown in Figure 5(a) was performed as follows: When all of the "catastrophic" data points were processed as failures, the others in the group were treated as "suspensions." The process was switched with all "slow degradation" failures processed as failures and all "catastrophic" ones treated as suspensions. As a result, the original mixed TTF data set was separated into "catastrophic" and "slow degradation" subsets that were modeled separately. Figure 5(b) shows the corresponding contour plots of the two subsets. It is clear that the two data sets have different β and η values and must be *statistically* considered as two independent failure modes.

Figure 6 shows the Weibull probability plot of the TTF data from Table II. Arrows are used to indicate the data points that failed "catastrophically." One obvious difference between the Weibull plots of Figures 5(a) and 6(a) is that the data points shown in Figure 6(a) did not reveal a mixture of data points with two distinct β values. Indeed, all data points in Figure 6(a) appear to fit a single Weibull distribution. However, if the same modeling approach that was used for distinguishing MTTF data in Figure 5(a) is also applied for the data from Figure 6(a), two

completely separate contour plots also are revealed [Figure 6(b)]. This is clear evidence that the data points shown in Figure 6(a) that appear to fit a single Weibull plot actually fit two separate failure modes much better.

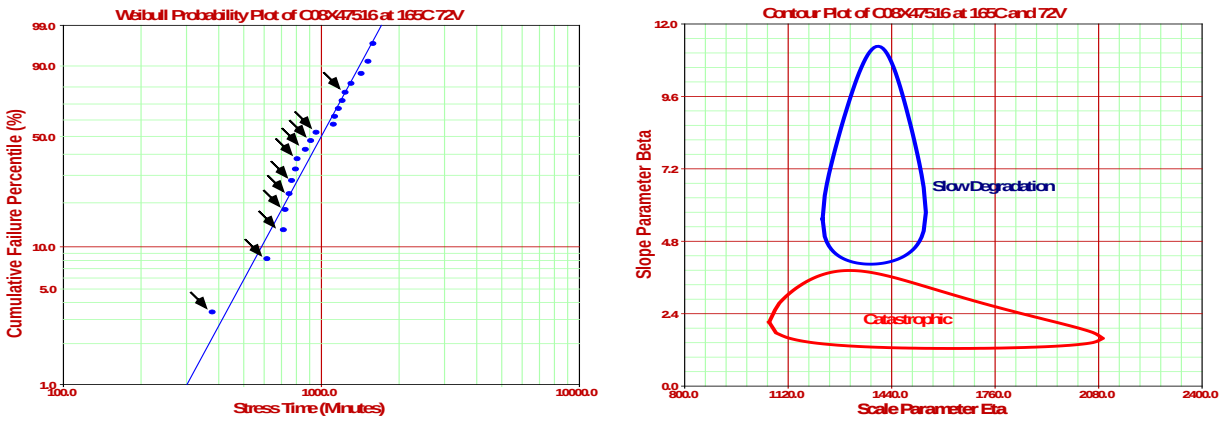

(a) (b)

Figure 6. Weibull modeling results of TTF data from Table II for BME capacitor C08X47516, life tested at 165°C and 72V. (a) Weibull plot, with arrows indicating all catastrophic failures. (b) Contour plot reveals the two slope parameters β for the two different failure modes, but the two subgroups share a similar scale parameter η.

The fact, shown in Figure 6, that a single failure mode-like Weibull distribution can actually be divided into two separate failure modes when the leakage current data is taken into account (two separate contour plots) represents a real confusion and challenge during the Weibull modeling of MTTF data for many BME capacitors. It is essential that leakage current measurements be used to distinguish the different failure modes in order to establish a realistic reliability model for BME capacitors.

Acceleration Factors of BME Capacitors

As summarized in Table I, three different acceleration factors have been considered for modeling BME capacitors with respect to external electric field. Figure 7(a) shows the MTTF data as a function of applied external field ($E = V/d$) at a constant temperature of 165°C for a number of BME capacitors, including the previously reported data [6] and the published MTTF data of a 0603 medical-grade BME capacitor with an X7R dielectric [5].

The MTTF data in Figure 7 are both curve fitted by a power-law form described by a *P*-*V* equation [Eq. (3)], and by an exponential form (*E*-model), as shown in Table I. The results reveal that all MTTF data can be fit to the exponential law better than to the power law, as indicated by the fact that smaller R^2 values are always obtained when the same data points are curve fitted using a power-law form. The results shown in Figure 7 suggest that MTTF data for most BME capacitors may not follow the expected power law [Eq. (3)] when exposed to an external electric field.

In order to better understand this issue, the MTTF data as a function of electric field were re-plotted with respect to the failure modes. Figure 8 shows the MTTF data against electric field at a constant temperature (165°C). The MTTF data showing in Figure 8(a) include only the Weibull modeling results from units with slow degradation failures, as distinguished by leakage current measurement. The remaining units were modeled as suspensions. The MTTF data in Figure 8(b) are the opposite of the results showing in Figure 8(a). For slow degradation failures, exponential curve-fitting always gives rise to higher R^2 values [Figure 8(a)], and for catastrophic failures, power law always results in higher R^2 values [Figure 8(b)]. The difference in R^2 is fairly small, but there are no exceptions! It is expected that the difference in R^2 for the two failure modes will become more distinct when more MTTF data points are available, particularly at lower electrical fields, although this may take years of testing to prove [19].

If we assume that the fact shown in Figure 8 is true, i.e., MTTF of a slow degradation failure follows exponential law, and that of a catastrophic failure follows power law, it will be useful to answer some questions about the exponential behaviors shown in Figure 7(b) for BME capacitors.

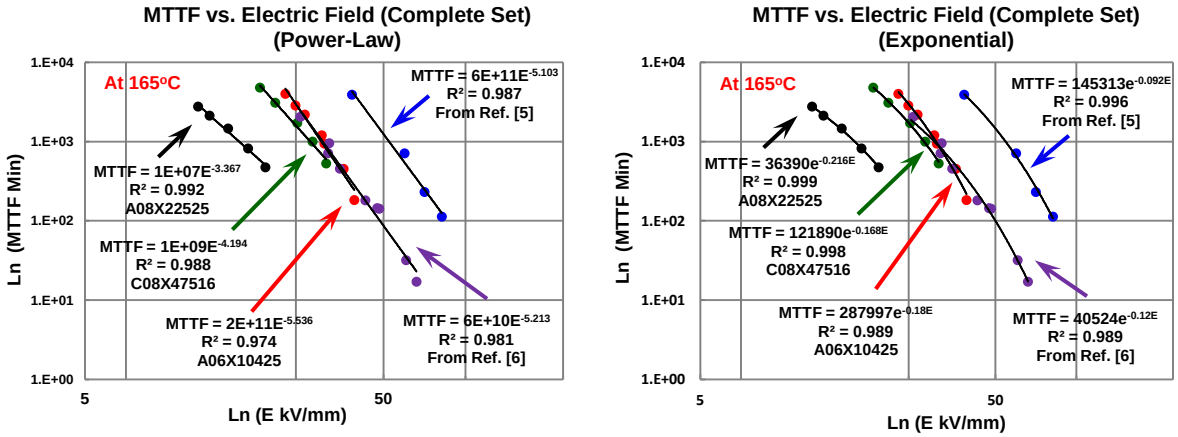

(a) (b)

Figure 7. MTTF as a function of applied external electrical field for BME capacitors: (a) curve fitting to MTTF data determined using a power law; (b) curve fitting of MTTF data with an exponential law.

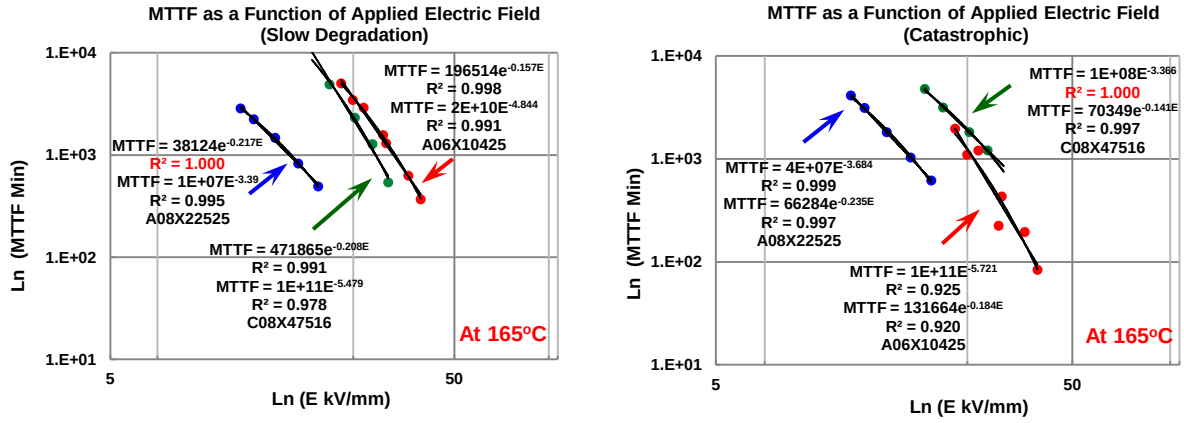

(a) (b)

Figure 8. MTTF data as a function of applied electric field at 165°C for BME capacitors with slow degradation failures (a), and with catastrophic failures (b).

(1) Why do most PME capacitors follow the power law dependence on *E*? It has been true for several decades that traditional PME capacitors with $BaTiO_3$ dielectrics follow the power law as defined in the P-V equation [Eq. (3)]. This is because slow degradation failures are due to the electromigration of oxygen vacancies, which has never been an issue in PME capacitors. This also explains why all PME capacitors failed in a catastrophic mode (either avalanche or thermal runaway). However, when the accelerated life stresses went high enough, a deviation from the power-law relationship was observed for PME capacitors due to the anomaly in leakage current [1].

(2) Why does the MTTF of most BME capacitors exhibit an exponential dependence on *E*? We can assume that at a given temperature and applied field, all failures are catastrophic, and there are no slow degradation failures. With an increase of the field, a number of slow degradation failures will appear. As shown in Figure 1, slow degradation failures had a relatively longer TTF than catastrophic failures. As a result, the MTTF, which is a simple average of all TTF values, will increase with an increasing electric field. On the other hand, the values of τ_{SD} have been found to decrease with an increasing electric field. At a certain electrical field value, the small τ_{SD} will result in most BME capacitors failing by slow degradation prior to the occurrence of any catastrophic failures. At this point, the MTTF of the slow degradation failures will be smaller than that of only catastrophic failures. As shown in Figure 7 (a) and (b), if the MTTF data of power-law failures represents a straight line, the introduction of slow degradation failures

with decreasing failure time (τ_{SD}) and an increasing field will form a curvature in MTTF data vs. electrical field. This curvature will fit an exponential law better. The decrease of τ_{SD} with an increase in electrical field has been found to be true for all BME capacitors that reveal slow degradation failures.

(3) The slow degradation failures that follow an exponential acceleration factor also agree with the observed fact that the leakage current vs. stress time for slow degradation failures also fits an exponential law [Eq. (10)].

As a result of this study, the observation that MTTF of many BME capacitors appears to fit exponential law better over the power-law is due to the combination of two failure modes: one follows the exponential; the other follows the power law.

Reliability Lifetime Verification Using HALST Results

Figure 9(a) shows the Weibull plots of TTF data obtained under various stress conditions. The data appear to fit well to a single Weibull distribution since no significant changes in β values are revealed among Weibull plots under various stress conditions. A TTF data set taken at 135°C and 72V is also included in the plot for the purpose of modeling verification; it will be discussed later. The "normalized" Weibull probability plots at 125°C and 32V (twice the rated voltage) are shown in Figure 9(b) for three different failure scenarios, in which each data point is extrapolated from Figure 9(a) using a most likelihood estimation (MLE) method and a power-law acceleration factor (*P-V Equation*). This is done for each failure and for any suspensions that are entered, and then the median ranks of the failures are determined. More details on this approach for characterizing HALST results have been described previously [6, 7].

A total of three normalized Weibull plots were generated due to the existence of two distinct failure modes that were revealed in leakage current measurements, and a mixture of both. The plot labeled "complete set" is the normalized Weibull plot that all TTF data points showing in Figure 9(a) were used for modeling, except the data set of 135°C, 72V. This plot also represents a conventional Weibull plot when all of the units are assumed to fail with only a single failure mode. The "catastrophic" plot is created using all of the data points that failed with a catastrophic characteristic and with all remaining data points (that failed with slow degradation) set as suspensions. The slow degradation plot is one in which only slow degradation failed samples were used for Weibull modeling and those that failed "catastrophically" remain suspensions.

The three plots predict reliability life for three scenarios: catastrophic, slow degradation and mixed together. It is noticeable that the three Weibull modeling plots give rise to different scale parameters η, indicating that each model predicts a different reliability lifetime. The three separate Weibull reliability plots can also be generated when the different acceleration factors shown in Table I are selected. As a result, the measured TTF data under various stress conditions as shown in Figure 9(a) will eventually give rise to a total of 9 different reliability lifetime results when the HALST modeling method described in this study is applied.

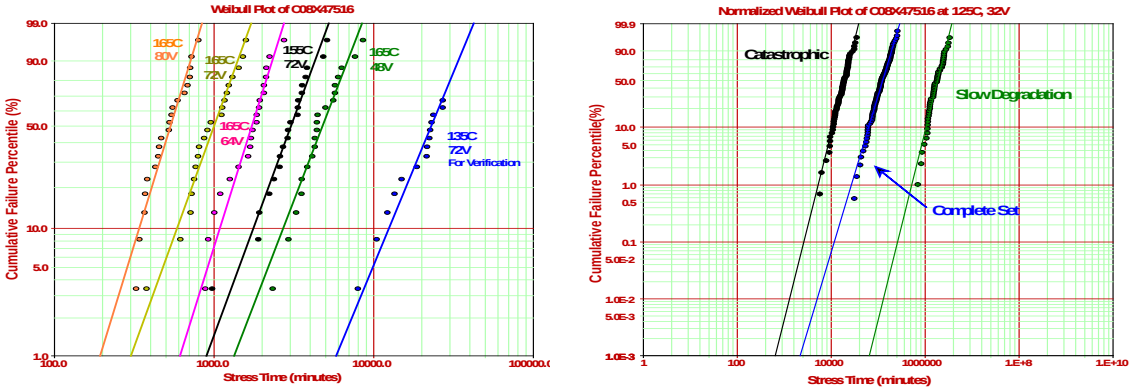

(a) (b)

Figure 9. Weibull plots for BME capacitor C08X47516 under various stress conditions (a); corresponding normalized probability plots at 125°C and 32V, with a power-law acceleration factor (b).

Table III summarizes the calculated MTTF results as a function of failure modes (plus a traditional mixture of two failure modes) and three possible acceleration factors at a stress level of 135°C and 72V. The calculated MTTF data are highly dependent on the acceleration factors and failure modes. The exponential form gives rise to the smallest MTTF results for all failure modes and is thus the most aggressive acceleration factor for this capacitor. The catastrophic failure yields the lowest reliability life among the various failure modes.

Table III. Calculated MTTF (hrs) Data of C08X47516 at 135°C and 72V for Model Verification

	Acceleration factors		
Failure Modes	E-Mode (Exponential)	Power Law	E-Mode (High Stress)
Complete Set (mixed)	427.10	2111.17	2778.67
Slow Degradation	9438.50	30835.00	52335
Catastrophic	79.86	318.67	381.65
Measured Verification Data	318.28		

The measured verification data in Table III were directly derived using Eq. (2) when measured TTF data at 135°C and 72V were used to fit a *2*-parameter Weibull distribution to determine β and η values. This process does not involve any acceleration factors. The MTTF data for the complete set in Table III were calculated by using all data points that were assumed to fit a single failure mode, which corresponds to the calculated reliability life when a traditional Weibull distribution of a single failure mode is used. It should be noted that MTTF data in Table III with a power-law acceleration factor use the same model as defined in Eq. (5) for PME capacitors. Clearly, the 2,000+ hours is well above the measured MTTF of 318.28 hours under this stress condition. The MTTF data of a complete set with an exponential *E*-mode are close to the measured data but are still longer. Indeed, the measured data fit best to the calculated MTTF data that assumes a catastrophic failure mode and a power-law acceleration factor.

Finally, as shown in Table III, the MTTF data calculated for slow degradation failures with power law, and those for catastrophic failures with *E*-mode are both not applicable, as revealed in Figure 8, slow degradation failures follow an exponential law, and catastrophic failures follow a power law.

If this prediction is true, then all of the capacitors that failed at 135°C and 72V should have had catastrophic failures and should have followed the power law. Figure 10 shows the actual measured leakage current data, and it is true that all capacitors had catastrophic failures. The plot in Figure 8(b) also confirms that MTTF data of catastrophic failures fit the power law better. The calculated MTTF results for other BME capacitors in this study also show similar results to those summarized in Table III.

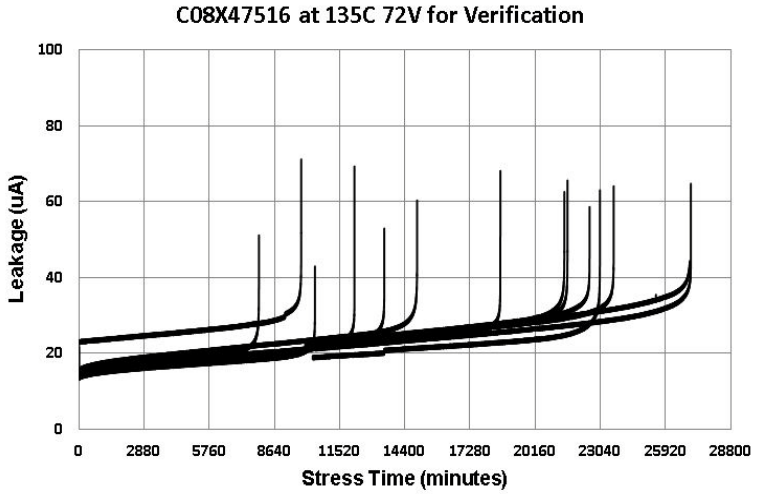

Figure 10. Leakage current results at 135°C and 72V confirms the proposed reliability model for BME capacitors.

Reliability Lifetime Prediction Using HALST Results

Although traditional highly accelerated testing often uses MTTF to characterize and predict a capacitor's reliability life, it has been realized that MTTF might be one of the most misunderstood metrics in reliability engineering. MTTF has been used to mean the lifetime at which 50% of the units of the population will fail, but this will only be the case if the distribution is normal, or symmetric. MTTF has also sometimes been defined as the reverse of the failure rate, but this is only correct if the distribution is exponential and the failure rate is constant. For Weibull distribution, the MTTF is defined as shown in Eq. (2). However, the MTTF will be altered if β and η change. When predicting reliability life, it is important to know the rate at which a population will fail. For better predicting the reliability life of BME capacitors, it is preferred that BX life shall always be used.

BX refers to the time by which *X%* of the units in a population will have failed. BX is better for defining the durability part of reliability for a population than MTTF for following reasons:

(1) BX life of a *2*-parameter Weibull can be calculated using Eq. (12). The BX life is not only related to the model parameters but also directly to the reliability $R(t)$ that is a function of time.

$$t_R = \eta \cdot \{-ln[R(t_R)]\}^{1/\beta} . \quad (12)$$

Where $R(t_R)$ = 1-*X%*, which corresponds to the probability that 1-*X%* units in the population have not failed at t_R. In addition, BX life or the reliability at a given time are more appropriate metrics because they can be calculated for any of the statistical distributions commonly used to analyze product lifetime data. As shown in Table IV, BX changes greatly with slope parameter β despite the retention of the same MTTF [20].

Table IV. A Comparison of MTTF to BX Life for a *2*-parameter Weibull Model

Slope Parameter β	Scale Parameter η	MTTF (minutes)	B1.0 (minutes)
1.0	10000	10000	101
2.0	11280	10000	1130
4.0	11030	10000	3490

(2) One of the biggest concerns in predicting the use-level reliability of $BaTiO_3$-based BME capacitors with highly accelerated life stress testing is that most data were measured above the phase transition temperature of $BaTiO_3$, around 120°C, whereas the use-level is assumed here as at room temperature (25°C) and rated voltage. This makes it very questionable that the action energy E_a and Weibull slope parameter β obtained above the phase transition temperature would be similar to that obtained at 25°C. An alternative for circumventing this problem would be to use BX life to predict the reliability of BME capacitors at 125°C and twice the rated voltage V_r.

MIL-PRF-123 requires that all PME MLCC inspection lots pass life test at 125oC and 2x V_r for 4,000 hours for qualification inspection. Based on the lot size, 125 capacitors are used for this specified life testing, with two failures (after 250 hours) acceptable. For evaluation for space applications, all 125 units must pass the life test. This requirement can be readily converted to a BX life of 4,000 hours at *X%* = 1/125 = 0.8% -- or, in other words, BME capacitor inspection lots must have a B0.8 ≥ 4,000 hours at 125oC and 2x V_r in order to be considered for space-level applications.

Table V summarizes the calculated B0.8 life at 125°C and 2xV_r for a number of BME capacitors and offers a comparison to actual measured B0.8 life that corresponds to the *first* failure in a life test group of 125 units. The results calculated using the model developed in this study agree with the testing data. Further use of BX life to evaluate the reliability of more BME capacitors is still in progress.

Summary

To solve the concerns and problems that are related to conventional highly accelerated testing of BME capacitors, a modified, advanced highly accelerated life stress test (HALST) was developed and used to evaluate and predict the reliability life of commercial BME capacitors.

Table V. Calculated B0.8 Life (hours) at 125°C and 2xV_r Comparisons to Measured B0.8 Life

BME Part Numbers	Failure Modes	Power Law	*E*-Model (Exponential)
C08X47516	Complete Set	103795	427
	Slow Degradation	51680000	9439
	Catastrophic	3096	80
	Measured (Failure mode)	**2998 (catastrophic)**	
A06X10425	Complete Set	8855167	82877
	Slow Degradation	22226667	203033
	Catastrophic	1429233	5427
	Measured (Failure mode)	**>4000 (no failure)**	
A08X22525	Complete Set	1155	1159
	Slow Degradation	1359	1385
	Catastrophic	948	881
	Measured (Failure mode)	**939 (catastrophic)**	

A general reliability function that includes the impact of external stresses, construction, and microstructure was proposed for BME capacitors. A combination of leakage current and MTTF measurements has been used to distinguish the failure modes and to separate the MTTF data into two groups: slow degradation and catastrophic. The slow degradation failures fit an exponential form Eq. (10) very well. A characteristic exponential growth time τ_{SD} was used to describe the reliability life of this failure. The larger the value of τ_{SD}, the longer the reliability of a slow degradation process.

Although the two failure modes identified may represent different stages of a dielectric wearout, the MTTF data have to be separated into two subsets when the *2*-parameter Weibull distribution is used for reliability modeling. When the catastrophic subset is used for reliability modeling, the data points from the slow degradation subset are treated as suspensions, and vice versa. As a result, there will be three Weibull modeling results for a given MTTF data set: completed (conventional), slow degradation, and catastrophic.

The MTTF of most BME capacitors reveal an exponential dependence on the applied electric field ($E = V/d$). However, when MTTD data were further divided and modeled separately for two failure modes, the initial MTTF data for slow degradation failures appear to follow the exponential law, and that for catastrophic failures appear to follow the conventional power law. This finding may help to answer the question of why most PME capacitors have a power law dependence, while BME capacitors have an exponential dependence over an electric field.

The developed reliability model, with respect to mixed failure modes and different acceleration factors, agrees with the measured HALST results -- not only the MTTF data, but also the failure modes (either catastrophic or slow degradation).

B0.8 life was used to predict the reliability life of BME capacitors at 125°C and 2x V_r, the condition that all MLCCs are subject to for at least 1,000 hours of life testing for consideration for high-reliability space applications. B0.8 life corresponds to the first unit that failed in a group of 125 BME capacitors. This approach can help to screen out the part numbers of a specific batch that may fail the potential life test. With this type of screening, the prerequisite expensive and tedious life testing at 125°C and 2x V_r can be used only for those BME capacitors that reveal the potential to pass the life test after evaluation using the quick turnaround HALST method described in this work.

Acknowledgements

The author appreciates the NASA Electronic Parts and Packaging (NEPP) program's support for this study and is especially thankful to Michael Sampson and Ken LaBel, the NEPP program managers, for their help and encouragement. The author also expresses his gratitude to Michael Sampson and Bruce Meinhold for reviewing the manuscript. The author would also like to thank the GSFC Code 562 Parts Analysis Laboratory for assistance with electrical testing.

References:

1. B. Rawal and N. Chan, "Conduction and Failure Mechanisms in Barium Titanate Based Ceramic Under Highly Accelerated Conditions," *Proceedings of Electronic Components Conference*, New Orleans, pp. 184, (1984)

2. J. L. Paulsen and E. K. Reed, "Highly Accelerated Lifetesting of Base-Metal-Electrode Ceramic Chip Capacitors," *Microelectronics Reliability*, **42**, pp. 815, (2002)
3. M. Randall, A. Gurav, D. Skamser, and J. Beeson, "Lifetime Modeling of Sub 2 Micron Dielectric Thickness BME MLCC," *CARTS Proceedings*, pp. 134, (2003)
4. D. Liu, H. Leidecker, T. Perry, and F. Felt, "Acceleration factors in Life Testing of High-Voltage Multilayer Ceramic Capacitors," *CARTS Proceedings*, pp. 45, (2005)
5. T. Ashburn and D. Skamser. "Highly Accelerated Testing of Capacitors for Medical Applications," *Proceedings of the 5th SMTA Medical Electronics Symposium*, (2008)
6. D. Liu and M. Sampson, "Reliability Evaluation of Base-Metal-Electrode Multilayer Ceramic Capacitors for Potential Space Applications," *CARTS Proceedings*, pp. 45, (2011)
7. D. Liu and M. Sampson, "Some Aspects of the Failure Mechanisms in $BaTiO_3$-Based Multilayer Ceramic Capacitors," *CARTS Proceedings*, pp. 59, (2012)
8. N. Kubodera, T. Oguni, M. Matsuda, H. Wada, N. Inoue, and T. Nakarama, "Study of the Long Term Reliability for MLCCs," *CARTS Proceedings*, pp. 77, (2012)
9. T. I. Prokopowicz and A. R. Vaskas, "Research and Development, Intrinsic Reliability, Subminiature Ceramic Capacitors," Final Report ECOM-90705-F, NTIS AD-864068, (Oct. 1969)
10. D. Hennings, "Multilayer Ceramic Capacitors with Base Metal Electrodes," *Proceedings of the 12th IEEE International Symposium* **1,** pp. 135, (2000)
11. J. M. Herbert, *Trans. Br. Ceram. Soc.* **63**, pp. 645, (1963)
12. Y. H. Han, J. B. Applyby, and D. M. Smyth, "Calcium as an Acceptor Impurity in $BaTiO_3$," *J. Am. Ceram. Soc.***70**, pp. 96, (1987)
13. J. F. Scott, B. Melnick, L. McMillan, and C. Paz de Araujo, "Dielectric Breakdown in High-e Films for USLI DRAMs," *Integrated Ferroelectrics*, **3**, pp. 225, (1993)
14. J. F. Scott, "The Physics of Ferroelectric Ceramic Thin Films for Memory Applications," *Ferroelectrics Review*, **1**[1], pp. 65, (1998)
15. J. McPherson and H. Mogul, "Underlying Physics of the Thermo-chemical E Model in Describing Low-Field Time-Dependent Dielectric Breakdown in SiO_2 Thin Films," *J. Appl. Phys.* **84**, pp. 1513, (1998)
16. J. McPherson and R. Khamankar, "Molecular Model for Intrinsic Time-Dependent Dielectric Breakdown in SiO_2 Dielectrics and the Reliability Implications for Hyper-Thin Gate Oxide." *Semiconductor Science and Technology* **15**[5], pp. 462, (2000)
17. J. W. McPherson, *Reliability Physics and Engineering: Time-to-Failure Modeling* (Springer, New York, 2010)
18. R. Weachock and D. Liu, "Failure Analysis of Dielectric Breakdowns in Base-Metal Electrode Multilayer Ceramic Capacitors," *CARTS Proceedings*, pp. 151, (2013)
19. J. McPherson, V. Reddy, K. Banerjee, and H. Le, "Comparison of E and 1/E TDDB Models for SiO_2 Under Long-Term/Low Field Test Conditions," *Proceeding on IEDM*, pp. 171, (1998)
20. D. Ryu and S. Chang, "Novel Concepts for Reliability Technology," *Microelectronics Reliability*, **45**[3], pp. 611, (2005)